

THE INSTITUTE OF PAPER CHEMISTRY, APPLETON, WISCONSIN

IPC TECHNICAL PAPER SERIES

NUMBER 269

**USING NEOPRENE-FACED, PVDF TRANSDUCERS TO COUPLE
ULTRASOUND INTO SOLIDS**

C. C. HABEGER, W. A. WINK, AND M. L. VAN ZUMMEREN

JANUARY, 1988

Using Neoprene-Faced, PVDF Transducers to Couple Ultrasound into Solids

C. C. Habeger, W. A. Wink, and M. L. Van Zummeren

**This manuscript is based on results of IPC Project 3467 and has been
submitted for consideration for publication in the
Journal of the American Acoustical Society**

Copyright, 1987, by The Institute of Paper Chemistry

For Members Only

NOTICE & DISCLAIMER

The Institute of Paper Chemistry (IPC) has provided a high standard of professional service and has exerted its best efforts within the time and funds available for this project. The information and conclusions are advisory and are intended only for the internal use by any company who may receive this report. Each company must decide for itself the best approach to solving any problems it may have and how, or whether, this reported information should be considered in its approach.

IPC does not recommend particular products, procedures, materials, or services. These are included only in the interest of completeness within a laboratory context and budgetary constraint. Actual products, procedures, materials, and services used may differ and are peculiar to the operations of each company.

In no event shall IPC or its employees and agents have any obligation or liability for damages, including, but not limited to, consequential damages, arising out of or in connection with any company's use of, or inability to use, the reported information. IPC provides no warranty or guaranty of results.

Using neoprene-faced, PVDF transducers to couple ultrasound into solids

C. C. Habeger, W. A. Wink, and M. L. Van Zummeren

The construction of PVDF transducers, designed for nondestructive testing on low-impedance solids, is described. These transducers are provided with soft neoprene front-faces so that efficient acoustic coupling can be realized without resorting to viscous coupling, epoxied interfaces or fluid immersion. This allows porous materials to be rapidly tested with no alteration in their acoustic properties. The benefits and limitations of neoprene coupling are discussed. Experimental results are presented to help establish conditions for the proper utilization of this coupling technique.

INTRODUCTION

Our reasons for writing this report are to (1) document the development of a low impedance, broad-band transducer, (2) discuss the use of soft neoprene for coupling dilatational waves into solids, and (3) present experimental results on the effects of loading pressure, surface roughness, and interface cleanliness on the quality of ultrasonic coupling between soft neoprene and solids. However, we begin with a brief description of the circumstances that stimulated our interest in coupling ultrasound with neoprene.

The purpose of our research is to find better ways of using ultrasound for the nondestructive testing of the out-of-plane viscoelastic coefficients of paper.¹⁻³ That is, we would like to accurately measure the phase velocity and loss coefficient in the thickness direction of paper. Since paper is a thin, rough, porous material made from wood pulp fibers which are irregularly shaped and highly variable, this is a formidable task. Wood fibers are multiple-layer, filament-wound structures which have a much larger axial than transverse modulus. When formed into a sheet, the fiber axes are aligned nearly in-plane, causing paper to be very mechanically anisotropic. As a result, the phase velocity of out-of-plane dilatational waves is only about 300 m/s, while in-plane velocities are around 3000 m/s. Out-of-plane velocities are highly sensitive to changes in the furnished pulp and to changes in manufacturing conditions. Since out-of-plane velocities can easily vary 20 to 30% on production from a single machine, velocity measurements with uncertainty of a few percent are valuable indicators of mechanical integrity. The shape of the pores in paper is governed by the dimensions of the fibers which can be loosely described as cylinders with diameters of 10 to 50 μm . Since the thickness of paper is from about 50 to 1000 μm ,

we must often work with samples which are less than an order of magnitude thicker than their pore dimensions. This means that we cannot use high frequency pulses to resolve the short transit times because wavelengths would be the order of the pore dimensions and scattering would be excessive. Since paper rapidly attenuates ultrasound over a few megahertz, our transducers are designed to operate at about 1.0 MHz, and paper thickness is often less than one wavelength.

To compound our problems, the nature of paper precludes the use of standard techniques for coupling ultrasound. Viscous fluids and epoxy are unacceptable coupling agents, as they penetrate the porous structure and grossly alter acoustic properties. Immersion testing is inappropriate, since many liquids are sorbed by wood fibers, expanding the paper and changing its mechanical properties. If a nonwetting liquid is used, the propagation of the dominant acoustic mode, which is concentrated in the fluid, is insensitive to the mechanical properties of the paper. For these reasons, an unconventional coupling procedure must be employed.

Conducting ultrasonic testing without a coupling agent causes many difficulties. The reflection coefficient between the bare transducer and sample is unduly large, and acoustic energy is inefficiently transferred. The coupling, which is affected by variabilities in surface and loading conditions, is not reproducible. Not only is the transferred signal amplitude greatly reduced, but coupling dependent phase shifts are experienced. Measurements which use the values of the sample interface reflection or transmission coefficients to calculate sample coefficients are severely jeopardized.

For out-of-plane testing in paper, a soft neoprene interface is a compromise between a standard couplant that alters paper properties and a poorly

coupled direct connection. That neoprene interface does significantly reduce interface reflection is supported by the observation that the signal amplitude through a paper sample is an order of magnitude higher when neoprene interfaces are inserted. Also, transmission is less influenced by surface roughness. As will be discussed later, the coupling is still imperfect at low loading pressures, and care must be taken in interpreting results. However, in the case of paper, where approximate measures of out-of-plane properties are useful, neoprene coupling is a critical improvement.

Although we are most interested in the testing of paper, we feel that neoprene coupling has broader implications. The application of neoprene faced transducers to test pieces is rapid and convenient. This is especially true when compared with epoxying the interfaces, using viscous couplants, or immersing in a fluid. As will be argued, neoprene coupling, administered by a suitable instrument at sufficient loading pressure, can be quite good when the surfaces are clean and smooth. In addition, neoprene is nearly incompressible and thereby does not effectively transfer transverse waves. Therefore, relatively pure dilatational wave propagation can be achieved.

I. TRANSDUCER DEVELOPMENT

We designed the neoprene-faced transducers used in this study to be broad-band and to have low mechanical impedance. It is essential that they are broad-band, since we intend to use them for pulsed ultrasonic testing of paper. The pulse must be short so that a discrete signal, which contains no interference from multiple reflections off the paper surfaces, is discernible. Low impedance transducers are needed for efficient out-of-plane coupling to paper. For these reasons, we chose polyvinylidene fluoride (PVDF or Kynar) film as the

piezoelectric medium. It has a lower mechanical quality factor than standard ceramic piezoelectrics (making it easy to build broad-banded transducers) and a much lower mechanical impedance.

The final configuration of a transducer is shown schematically in Fig. 1. The piezoelectric material is standard 110 μm thick PVDF film with nickel-silver electrodes procured from Pennwalt Corporation. The active element is a stack of four films bonded with a very thin layer of conductive epoxy. The two films on the top of the stack have one polarity, while the two bottom films are turned in the other direction. The center of the stack is connected to the transducer electrode, while the top and bottom surfaces are grounded. This effectively produces two films which are 220 μm thick and electrically parallel. The resulting structure is an approximately 440 μm piezoelectric element with a well shielded electrode.

Figure 1 here

The bottom of the stack is bonded (again with a very thin layer of epoxy) to a piece of unpolarized Kynar. This provides a good mechanical impedance match with the film stack thereby reducing backside reflections, suppressing resonances, and increasing transducer bandwidth. Mounting to the brass housing is also accomplished through the Kynar backing. Kynar is a good attenuator of acoustic energy and helps isolate the piezoelectric element from the brass frame. The top of the stack is bonded to a polystyrene disk. The polystyrene acts as a low-loss, impedance matching layer between the PVDF film and the neoprene face of the transducer. A brass retaining ring confines the lateral expansion of the neoprene when under pressure. This creates a relatively thick neoprene delay line with the compressibility of a thin neoprene layer. The

polystyrene and neoprene disks are thick enough that a few microseconds must elapse before a multiple reflection can reverberate. The transducers can therefore generate a distinct, microsecond-long pulse which is free of interference from reflections.

To reach high coupling pressures without overly large loads, similar transducers with 3/8-inch diameters were constructed. In addition, we also built 1-inch diameter transducers using a new PVDF copolymer (VF2-VF3 from Pennwalt) that has a larger piezoelectric coupling coefficient. These transducers were made with only two 110 μm films in the stack in order to decrease the pulse width. Figure 2 is a photograph of expanded oscilloscope traces of the primary pulses generated when two transducers were directly coupled. The transmitter was excited with a one-cycle 1.0 MHz burst. The top trace represents the signal from the standard PVDF transducers, while the bottom trace corresponds to the copolymer transducers. The oscilloscope gain for the standard transducers signal was twice the gain used for the copolymer transducers. In short, the copolymer film produced higher frequency transducers with greater sensitivity.

Figure 2 here

Manufacture of the critical components of a transducer begins by machining the polystyrene and Kynar cylinders to the overall dimensions shown in Fig. 1. After end facing, a cylinder is mounted off-center in the chuck of a lathe, and two small wedge-shaped sections are machined from its rim to accommodate lead attachment. Once the cylinders are complete, the PVDF film is sectioned into squares slightly greater than 1.0 inch on a side. Next, the neoprene disk is cut out of a 1/8-inch thick sheet of 5-10 durometer "super soft neoprene" made by Crane Packing Co. Since conventional cutting and stamping procedures

tend to produce bowed edges when used on neoprene, a special technique was developed to produce neoprene disks with uniform diameters. The neoprene is mounted on the face plate of a lathe with double-faced tape. A sharp flake from a razor blade is held off-center in the tail stock of the lathe. With the lathe turning, the flake is slowly turned into the neoprene, and a uniformly round disk is produced.

For assembly, the Kynar cylinder is placed in an alignment fixture. A metered amount of conductive epoxy (TRA-CON BA-2902) is deposited on the center of the top face. Epoxy dabs are also applied to the foil squares which are now stacked onto the Kynar cylinder. The polystyrene cylinder is placed in the alignment fixture atop the stack. One wedge-shaped gap aligns with a gap in the Kynar; the other does not. An 8 pound load is placed on the polystyrene cylinder. The edges of the foils are taped to opposite cylinders at the aligned gaps in order to expose a v-shaped cavity. Additional epoxy is placed in the v-shaped cavity and in the other two gaps. The epoxy is allowed to cure, and the Kynar-foil-polystyrene juncture is machined to a radius slightly under that of the original cylinder. Small grooves are machined into the epoxy that fills the three gaps. The same conductive epoxy is used to bond copper lead wires into the grooves. A uniform layer of Loctite Black Max adhesive is applied to the top face of the polystyrene cylinder. Using a centering guide, the neoprene is laid on top and loaded with a 200 gram mass. The adhesive is allowed to set, and the transducer stack assembly is complete.

III. EXPERIMENTAL APPARATUS

Figure 3 is an operational schematic of our equipment. The mechanical portion of the apparatus is a paper caliper instrument^{4,5} modified to hold the transducers. One transducer is fixed to the anvil of the caliper gage. The

other is mounted to the pressure foot which is attached to graphite pistons that slide in a precision-bore glass tube. This allows the transducer friction-free axial motion with tight lateral constraint. Using thin shims, the transducers are carefully aligned in the caliper gage so that their housings are parallel and vary in separation by less than 2 μm . The pressure foot can be raised and lowered by a computer controlled motor. When lowered, the load on the transducers is determined by the dead-weight of the pressure foot and top transducer. Transducer pressure is adjusted by adding weights to a platform on top of the pressure foot or to counterbalances connected by pulleys to the pressure foot. An L.V.D.T. core is in a probe mounted in the pressure foot; the L.V.D.T. coils fit around the glass tube. An A.C. signal from the L.V.D.T. is amplified, detected, and sent to a digital voltmeter. The voltmeter is interfaced to the computer over an I.E.E.E. bus.

Figure 3 here

The transducers are normally operated in a transmitter-receiver configuration. The transmitter is driven by a R.F. power amplifier which is excited by a single cycle sinusoidal wave from a function generator. The repetition rate of the transmitter burst is set by another function generator used as a free-running pulse generator. The repetition rate (usually about 2 kHz) is chosen as large as possible without multiple reflections from the previous burst interfering with the primary pulses. The pulse generator also triggers a digital oscilloscope that displays the time history of the amplified receiver signal. An AT class personal computer monitors the digital voltmeter, controls the pressure foot, and analyzes the receiver signal.

The measurements which we will report are made in the following manner. The instrument is first calibrated for thickness measurements. This is done by

recording the L.V.D.T. output for two metal shims of known thickness and doing a linear interpolation of later L.V.D.T. readings to calculate sample calipers. An L.V.D.T. reading is initiated when the computer activates the motor to lower the pressure foot on a sample placed between the transducers. After a programmed time delay of 5.0 seconds, the computer reads and records the output of the digital voltmeter. It is important that the computer controls the motor driven lowering of the pressure foot, as this insures that the time-dependent coupling of the neoprene to the sample is repeatable.

After caliper calibration is complete, an acoustic "reference signal" is recorded. The reference is an eight-micron-thick aluminum foil. Once it is inserted into the span between the transducers, the jaws are closed. After the 5.0 second delay, the computer directs the oscilloscope to digitize the receiver signal. The trigger pre-delay of the oscilloscope has been set so that there is an expanded view of the main pulse. The oscilloscope does a 10 bit analog to digital conversion of 501 data points. One data point is digitized on each of 501 consecutive repetitions of the receiver signal. The effective digitization rate on the repetitive signal is 125 MHz. The signal is transferred to the computer over the I.E.E.E. bus. The signal length is then artificially increased to 512 points by repeating the last data value eleven times, and this signal is stored in computer memory for later comparison to sample signals. A Fast Fourier Transform algorithm is performed on the reference signal, giving phase and amplitude numbers for integer multiples of 0.2441 MHz. The signal is graphed on the computer C.R.T. display.

The reader may wonder why neoprene to neoprene coupling was not used for the reference. When a neoprene disk is pressed against another identical neoprene disk, the sides of the combined structure bulge out in a single arc

with the maximum lateral expansion at the interface. However, when a neoprene disk is pressed against a solid with more lateral rigidity, the bulge maximum is at the center of the disk. The neoprene has greater normal compression and greater lateral expansion when pressed to neoprene than when pressed to a conventional solid. It is important that the neoprene be in the same state at the reference condition and during sample testing. Therefore, a thin reference foil is used to constrain the neoprene bulging, and a correction is made for the small acoustic delay through the foil. As will be apparent later, the calculation of the reference delay is more involved than might be first thought.

Sample testing begins by inserting the specimen and closing the jaws. A receiver signal with no trigger pre-delay and a long time base is recorded. The computer does a crude analysis of the signal to determine an appropriate trigger pre-delay. Now testing starts in earnest. The pressure foot is raised and lowered. After 5.0 seconds, the digital voltmeter output is recorded, and the sample signal is digitized, extended, and stored. The sample signal is displayed on the C.R.T. below the reference signal. The computer calculates a "cross correlation delay time" by finding the offset time that maximizes the convolution integral of the reference and sample signals. The sample signal display is shifted by the cross correlation delay time to demonstrate the optimum signal alignment. The "cross correlation velocity," which is defined as the measured sample caliper divided by the cross correlation delay time plus the foil delay time, is calculated. Next, a Fast Fourier Transform is performed on the sample signal. In the event the operator notices that a reflection encroaches into the 512 data points, windows on the signal can be adjusted from the keyboard to limit the range of the F.F.T. Taking into account the different trigger pre-delays, the sample frequency domain amplitude and phase numbers are

referenced to the corresponding foil values. The phase values are corrected by 2π times the integer that causes the phase velocity at that frequency to be nearest the cross correlation velocity. The pressure foot is raised and the sample can be shifted to test at a new location. The pressure foot falls, and a new signal is analyzed. This process is repeated an adjustable number of times. The calipers, cross correlation velocities, and frequency domain numbers are averaged, and the results are printed.

IV. IMPEDANCE DETERMINATIONS

In order to evaluate neoprene coupling, it is first necessary to determine the acoustic impedances of the neoprene and the test specimens. The specimens used in the evaluation are made of aluminum, polystyrene, and unpolarized Kynar. Aluminum was chosen since it could easily be obtained in thin foils of different thicknesses. Polystyrene and Kynar are examples of low and high loss plastics and are important in the construction of our transducers. The acoustic properties of the rolled aluminum were taken from reference texts. They are $\rho = 2695 \text{ kg/m}^3$, $c = 6420 \text{ m/s}$, and $Z = 1.730 \cdot 10^7 \text{ kgm}^2/\text{s}$. Here, ρ represents the mass density; c is the velocity of dilatational waves; and Z is the acoustic impedance of dilatational waves. The properties of the other materials were measured.

A through-transmission technique was used to measure the acoustic properties of the plastics. Flat samples of different thickness were placed between the transducers, and the values of the phase and amplitude of the received signals were compared. There are, of course, unknown phase and amplitude shifts at the plastic-neoprene interfaces. However, our instrument applies the neoprene to the samples in a repeatable manner, and we assume that the comparison cancels

the interface effects. The plastic pieces were machined and polished to a sufficient thickness to guarantee that the straight-through pulse is complete before the first multiple reflection in the plastic can interfere. The polystyrene thicknesses are 2476 and 6259 μm , and the Kynar thicknesses are 2705 and 6319 μm . The mass densities (1049 kg/m^3 for polystyrene and 1766 kg/m^3 for Kynar) were found by weighing regular shaped specimens.

The amplitudes and phases of the Fourier components of the primary pulse were measured on the plastic samples at loading pressures of 50, 79, 137, and 362 kPa. Before determining the acoustic properties, corrections were made for diffraction effects in the amplitudes and phases of the signals through the plastic samples. This was done by assuming that the transducers move uniformly in and out as a piston, and by using diffraction correction curves published by Papadakis.⁶ The phase differences and ratios of the amplitudes were then used to calculate the phase velocities and loss tangents at 0.73, 0.98, 1.22, 1.47, and 1.71 MHz and at all loading pressures. The results for polystyrene were independent of pressure and frequency. The average value of the phase velocity was 2305.6 m/s with a standard deviation of 3.6 m/s, and the average loss tangent was 0.0012 with a standard deviation of 0.0014. The diffraction correction had lowered the phase velocity by 4 m/s, but it had a large relative effect on the loss tangent. Without diffraction correction the loss tangent would have been 0.0038 ± 0.0016 . Since the diffraction corrected loss tangent is smaller than its variability and its diffraction correction, we assume for later calculations that the acoustic loss in polystyrene is negligible, the phase velocity is 2306 m/s, and the impedance is $2.418 \times 10^6 \text{ kg/m}^2\text{s}$. For Kynar the loss tangent numbers were significant. The mechanical properties were dependent on frequency, but independent of loading pressure. The results are in Table 1.

TABLE I. The frequency dependent acoustic parameters of Kynar.

Frequency, MHz	Velocity, m/s	$\tan\delta$	Impedance, $10^6 \text{ kg/m}^2\text{s}$
0.7324	1957 ± 5	0.059 ± 0.008	$3.44 e^{i.030}$
0.9766	1971 ± 3	0.069 ± 0.006	$3.46 e^{i.035}$
1.2207	1985 ± 1	0.076 ± 0.006	$3.48 e^{i.038}$
1.4648	1995 ± 2	0.081 ± 0.005	$3.50 e^{i.042}$
1.7090	2004 ± 2	0.086 ± 0.004	$3.52 e^{i.043}$

The neoprene impedance determination began with a density measurement. A sample was weighed, and a mercury porosimeter was used to find its volume as a function of pressure. The neoprene was nearly incompressible; its density was 1108 kg/m^3 at atmospheric pressure and 1110 kg/m^3 at the top pressure of 27,000 kPa. For this work the density was therefore taken as 1108 kg/m^3 . To calculate the phase velocity, the signal through a 3.2-mm-thick neoprene sample sandwiched between two 8- μm aluminum foils was compared with the reference signal. The caliper was the computer calculated value less 16 μm . After making a small correction for the phase shift through one foil and correcting for diffraction, the phase velocity was computed as the caliper times the angular frequency divided by the sample phase shift less the reference phase shift. This was done at 50, 79, 137, 360, 707, and 2107 kPa and at the frequencies in Table I. The average of these 30 determinations was $1454 \pm 7 \text{ m/s}$. There was a slight increasing trend with frequency and pressure; however, this was ignored and the impedance was assumed to be $1.61 \times 10^6 \text{ kg/m}^2\text{s}$ at all conditions.

V. TRANSMISSION LINE EQUATIONS

Before we can quantify neoprene coupling, we need coupling dependent relationships for the phase shift and amplitude change of an acoustic wave

passing through a sample placed between two layers of neoprene. First, we will use standard transmission line equations to get "perfect coupling" results; then we will characterize less well bonded conditions. We will focus our attention on two limiting cases: (1) the sample transit time is greater than the pulse width, and we are only interested in the first transmitted pulse; and (2) the sample transit time is much less than the pulse width, and a discrete pulse resulting from the interference of all possible multiple reflections emerges.

When an acoustic wave is normally incident on an interface, part of the energy is reflected and part is transmitted. The ratio of the transmitted pressure amplitude to the incident pressure amplitude is the transmission coefficient, T . The reflection coefficient, R , is the ratio of incident to reflected pressure. Usually, the coupling is assumed to be perfect, and R and T can be derived from the impedances of the two materials. The perfect coupling conditions are: (1) there is a force balance at the interface or $1 + R = T$; and (2) the velocity is continuous across the interface or $1/Z_I - R/Z_I = T/Z_T$. Here Z_I is the dilatational acoustic impedance of the material in which the wave is incident and Z_T is that of the transmitted material. Solving these two equations for T and R gives the following well known relations.

$$T = 2Z_T / (Z_I + Z_T) \tag{1}$$

$$R = (Z_T - Z_I) / (Z_I + Z_T) \tag{2}$$

Using Eq. (1) and (2), we now find for case 1 the perfect coupling ratio, S_1 , of the outgoing amplitude to the incoming amplitude. Since we are ignoring multiple reflections, S_1 is simply the product of the neoprene to sample transmission coefficient, the sample propagation ratio, and the sample to neoprene transmission coefficient. That is, $S_1 = T_{NS} e^{-ikl} T_{SN}$, or in terms of the impedances

$$S_1 = 4e^{-ikl} / (2 + Z_S/Z_N + Z_N/Z_S) \quad (3)$$

In this equation, l represents the sample thickness, k is the sample wave number ($k = \omega/c$), ω is the angular frequency, the subscript N denotes the neoprene, and S denotes the sample.

Next we find S_2 . This is the same ratio; however, as the sample propagation time is now assumed to be much less than the pulse width, S_2 must include all the reflections. Summing an infinite number of components, S_2 is

$$\begin{aligned} S_2 &= T_{NS} T_{SN} (e^{-ikl} + R_{SN}^2 e^{-3ikl} + R_{SN}^4 e^{-5ikl} \dots) \\ &= T_{NS} T_{SN} e^{-ikl} / (1 - R_{SN}^2 e^{-2ikl}) \end{aligned} \quad (4)$$

Using Eq. (1) and (2) to put transmission and reflection coefficients in terms of impedances, produces Eq. (5).

$$S_2 = 4Z_S Z_N / [(Z_N + Z_S)^2 e^{ikl} - (Z_S - Z_N)^2 e^{-ikl}] \quad (5)$$

If r is defined as $(1 + R_{SN}^2) / (1 - R_{SN}^2) = 1/2(Z_N/Z_S + Z_S/Z_N)$, Eq. (5) simplifies to

$$S_S \approx e^{-irkl} \quad , \quad (6)$$

in the limit $rkl \ll 1$. This simply says that, for very thin samples, the neoprene-sample sandwich is equivalent to propagation (with no interfacial loss) through a sample of length rl . In other words, the signal is effectively reflected back and forth through the sample $(r - 1)/2$ times. Notice that the effective acoustic length of the thin sample increases with the impedance mismatch.

The above equations apply when the interfacial coupling is perfect. If slippage is allowed between the neoprene and the sample, the magnitude of the

transmission coefficient is less than stated in Eq. (1); the magnitude of the reflection coefficient is greater than stated in Eq. (2); and both coefficients experience a small additional phase. Since T_{SN} and T_{NS} are decreased, the first order effect is a decrease in the magnitude of S_1 . This is as expected: poor coupling results in less transmission of signal through a thick sample. The thin sample case is more interesting, as the results of poor coupling are not so intuitively obvious. The change in reflection coefficient greatly increases the value of r , and the first order effect in thin samples is an increase in the number of cross reflections and in the transit time. These two cases were chosen for study, since they allow us to look at situations in which the primary effect of poor coupling is either a signal loss or a phase shift.

When the coupling is imperfect, the above equations are no longer valid. In order to condense our results, we will characterize the coupling in terms of a single frequency-dependent parameter, $F(\omega)$. There are a number of ways that can be done. However, we chose the following one because it requires the introduction of only two very reasonable assumptions. The first assumption is that the force balance is maintained. That is, even with imperfect coupling, $l + R = T$. This means that we are ignoring any inertial terms associated with the connection between the two materials. The other assumption is that for each Fourier component of the signal the pressure is a complex number multiplied by the difference between the displacements of the two surfaces, or

$$l + R = T = F(\omega) (U_1 - U_2) \quad , \quad (7)$$

where U_1 is the displacement of the left hand surface, and U_2 is that of the right. This provides for frequency-dependent elastic and viscous elements in

the acoustic connection. Notice that we have allowed the surfaces to separate, and thereby modeled the interface as planes of different, but uniform, displacements. The perfect coupling limit is, of course, recovered as $F(\omega)$ approaches infinity.

Since $U_1 = (1 - R)/i\omega Z_I$ and $U_2 = T/i\omega Z_T$, we can use Eq. (7) to express T and R as functions of Z_I , Z_T , and $F(\omega)$. The results are

$$T = 2Z_T/[Z_I + Z_T + i\omega Z_I Z_T/F(\omega)], \quad \text{and} \quad (8)$$

$$R = [Z_T - Z_I - i\omega Z_I Z_T/F(\omega)]/[Z_I + Z_T + i\omega Z_I Z_T/F(\omega)] \quad . \quad (9)$$

For this model, poor coupling mandates the insertion of $i\omega Z_I Z_T/F(\omega)$ at appropriate places in the expressions for R and T . Therefore, we take CR , which we define as the absolute value of $i\omega Z_I Z_T/F(\omega)$ ($Z_I + Z_T$), to be a ratio which quantifies the relative effect of poor coupling. Later we will need poor coupling analogs of Eq. (3) and (5). These are generated by using Eq. (8) and (9), instead of Eq. (1) and (2), to calculate the values of T_{NS} , T_{SN} , and R_{SN} .

VI. EXPERIMENTAL RESULTS

Our first demonstration of the consequences of poor coupling is a comparison of measured time-of-flights for signals through aluminum foils. Since the two foils tested were thin (42.0 μm and 8.5 μm), the approximation, expressed in Eq. (6), is appropriate in the frequency range of interest. The impedance mismatch between the neoprene and aluminum is large ($r \approx 5.4$). Therefore, if the coupling is perfect, the received signal amplitude is unaffected by foil addition, and the time delay is the single foil transit time multiplied by 5.4. The time delay difference between the two foils would be about 28 nsec, and the two signals would have the same amplitude. The major impact of imperfect coupling is an extension of the transit times caused by the increase in R_{SN} .

Some of the results of our tests on aluminum foils are presented in Fig. 4. Time differences between the two foils are plotted on the y-axis. These were calculated by subtracting the phase of the 0.9766 MHz Fourier component in the pulse through the thin foil from that through the thick foil and converting the phase shift to a time difference. This was done at loading pressures from 50 kPa to 2100 kPa. In all cases, the computer was programmed to take the signal 5.0 seconds after the application of the load. Coupling does improve with contact time; however, for convenience, we used the 5.0 second delay because changes after this time are gradual.

Figure 4 here

The filled circles in Fig. 4 represent the calculated time differences assuming perfect coupling. The small variance with pressure is a result of the measured changes in neoprene impedance with pressure, which were included in these calculations. The hexagonal symbols just above the theoretical points are the measured time differences when the neoprene surfaces are "clean." The cleaning is a gentle, but thorough, rubbing with a damp cloth. The results above 500 kPa were taken using the smaller (3/8-inch diameter) transducers. Notice that at the lower pressures the imperfect coupling significantly increases the transit times. However, the discrepancy rapidly fades with loading pressure, and the difference between experiment and perfect coupling theory is within experimental error at the high pressures. The rest of the data in Fig. 4 demonstrates that surface contamination has a deleterious influence on coupling quality. Fiber lint was deposited on the neoprene surfaces by performing various numbers of tests on paper samples. The lower pressure results are badly compromised by dirtying the surface; but if sufficient pressure is applied, the coupling can be good even though the surface has been degraded.

We conducted other investigations into the influence of loading pressure on coupling quality by testing polystyrene and Kynar samples that were thick enough to justify the use of the case 1 assumption. These plastic samples were subjected to the test regime described in the "Experimental Apparatus" section. In addition, the computer was programmed to calculate the velocity and loss tangent for each Fourier component. In order to do this, the neoprene to sample transmission coefficients were calculated under the perfect coupling assumption. Using an iterative search technique for each Fourier component, a value of $\tan\delta$ and velocity were found that would produce the measured signal amplitude and phase shift if coupling were perfect. The first order effect of imperfect coupling on these measurements is to produce an overestimate of the loss tangent. The perfect coupling transmission coefficients are less than those experienced, and too much signal loss is attributed to acoustic attenuation in the plastic. There are also small phase shifts, induced by the imperfect coupling, that lead to velocity errors, but these are minor in comparison with the loss tangent difficulties.

The logarithms of the loss tangents at 0.9766 MHz, calculated for polystyrene samples, are plotted against pressure in Fig. 5. The loss at each surface in decibels necessary to account for the measured signal amplitudes is also marked along the y-axis. The filled circles represent the results for a smooth, 2476- μm thick specimen. The other data points come from measurements on pieces of nearly the same thickness, but with rough surfaces. These were created by cutting v-shaped, spiral grooves in the surfaces. The spacings of the grooves were adjusted so that a uniform, saw-toothed pattern was achieved. Since the loss tangent in polystyrene is about 0.01, the very large numbers calculated at low pressure and with roughened surfaces must be attributed to poor coupling.

Loading pressure rapidly improves coupling, but reasonable estimates of the actual loss tangent are not produced until the pressure is above 500 kPa on the smooth specimen. Figure 6 is an identical plot for Kynar samples. Again, the surface should be smooth and the pressure high to get a reasonable value for $\tan\delta$. The velocity determinations (not shown) were less affected by the poor coupling. The smooth surface results were within 0.1% above 500 kPa and within 1.0% at all pressures of the corresponding plastic velocities calculated earlier. Above 500 kPa, all data were within 1.0% of the expected values. In summary, for our case 1 experiments, poor coupling appears to induce attenuations that drown out the viscoelastic losses in the plastic samples and introduce time delays that are small compared with the transit times.

It is possible that some of the losses experienced with the serrate plastic samples could be attributed directly to surface roughness. That is, even with perfect coupling an irregular surface scatters energy and attenuates the specular portion of the transmitted wave. Recently, Nagy and Adler⁷ have published a method based on work done by Twersky,⁸ for estimating transmission losses due to a random surface roughness. Our serrate pattern does not make a random surface; however, applying the method of Nagy and Adler to our worst case (polystyrene with 50- μm grooves at 0.9766 MHz) gives an "effective phase modulation" of only 0.08. This produces a roughness generated loss of far less than 1.0 dB and can be easily ignored compared to the coupling losses.

Now that we have discussed the influence of neoprene coupling on case 1 and case 2 experiments, we will quantify the results by calculating the coupling factor, $F(\omega)$. First, we look at a case 2 comparison of signals through aluminum foils. Using Eq. (4), the ratio, r_{a1} , of the signal through a foil of thickness, L , to that of thickness, l , is

$$r_{al} = e^{-ik(L-1)} (1 - R_{SN}^2 e^{-2ikl}) / (1 - R_{SN}^2 e^{2ikL}). \quad (10)$$

Therefore, measuring the magnitude and phase of the ratio of signals through different foils allows us to determine the value of R_{SN} . By inverting Eq. (9), $F(\omega)$ is then calculated from R_{SN} . The results for a number of frequencies and loading pressures with clean transducers are listed in Table II.

TABLE II. Results of aluminum foil coupling experiments.

Frequency, MHz	r_{al}	R_{SN}	$1/F(\omega)$ $10^{-14} s^2 m^2 / kg$	CR
50 kPa				
0.732	$1.024e^{-i.142}$	$-0.847e^{i.046}$	$3.96e^{-i.13}$	0.267
0.977	$1.015e^{-i.199}$	$-0.851e^{i.036}$	$2.71e^{-i.37}$	0.243
1.221	$1.004e^{-i.255}$	$-0.854e^{i.033}$	$2.18e^{-i.51}$	0.245
1.465	$0.986e^{-i.310}$	$-0.857e^{i.029}$	$1.82e^{-i.63}$	0.245
1.709	$0.964e^{-i.363}$	$-0.859e^{i.026}$	$1.59e^{-i.73}$	0.250
79 kPa				
0.732	$1.013e^{-i.135}$	$-0.836e^{i.036}$	$2.70e^{-i.01}$	0.182
0.977	$1.004e^{-i.184}$	$-0.839e^{i.028}$	$1.71e^{-i.19}$	0.153
1.221	$0.993e^{-i.234}$	$-0.842e^{i.025}$	$1.31e^{-i.37}$	0.148
1.465	$0.978e^{-i.281}$	$-0.843e^{i.022}$	$1.05e^{-i.48}$	0.142
1.709	$0.958e^{-i.325}$	$-0.844e^{i.019}$	$0.85e^{-i.59}$	0.133
137 kPa				
0.732	$0.997e^{-i.134}$	$-0.834e^{i.014}$	$1.10e^{-i.25}$	0.074
0.977	$0.989e^{-i.182}$	$-0.838e^{i.013}$	$0.91e^{-i.52}$	0.081
1.221	$0.980e^{-i.227}$	$-0.838e^{i.014}$	$0.77e^{-i.50}$	0.086
1.456	$0.966e^{-i.272}$	$-0.840e^{i.013}$	$0.66e^{-i.61}$	0.089
1.709	$0.949e^{-i.316}$	$-0.841e^{i.013}$	$0.60e^{-i.73}$	0.095
362 kPa				
0.732	$0.988e^{-i.133}$	$-0.835e^{i.001}$	$0.38e^{-i1.30}$	0.025
0.977	$0.977e^{-i.178}$	$-0.836e^{i.000}$	$0.39e^{-i1.56}$	0.035
1.221	$0.965e^{-i.218}$	$-0.835e^{i.001}$	$0.26e^{-i1.48}$	0.030
1.465	$0.953e^{-i.258}$	$-0.835e^{i.001}$	$0.19e^{-i1.37}$	0.026
1.709	$0.937e^{-i.298}$	$-0.836e^{i.001}$	$0.20e^{-i1.37}$	0.031

There are points worthy of discussion in Table II. Notice, if CR is taken as the indicator of the relative degradation that poor coupling introduces,

it is clear that increasing loading pressure rapidly improves coupling. In fact, at the highest pressure (only 362 kPa), we barely have enough sensitivity to measure the influence of poor coupling. Also notice that the magnitudes of r_{a1} are greater than might be expected. Consider that each multiple reflection through a foil acquires an additional, thickness dependent phase shift. Thus, the reflectional components in the signal of a perfectly coupled thick foil should be further out of phase than those through a thin foil, and the signal through the thicker foil should have the lower magnitude. The magnitude of r_{a1} should be less than 1.0 and should decrease with frequency. Experimentally, the absolute value of r_{a1} does decrease with frequency; however, some of the low-frequency, low-pressure values are greater than 1.0. This is understood in terms of a small positive phase shift introduced into R_{SN} by imperfect coupling. This phase shift compensates for the propagation phase shift, and in some cases it allows the reflected components in the thick sample signal to be closer in phase than they are in the thin sample signal.

We also calculated the imperfect coupling values of R_{SN} , $F(\omega)$, and CR in the case 1 regime. This was done by taking the complex ratio of the Fourier components of the straight-through and the first-reflected signals in a polystyrene sample. This could be done on the 2476 μm specimen, since its thickness was intentionally chosen to produce discrete first transit and first reflected signals, which had no interference from internal transducer reflections. The reflected signal differs from the straight-through signal in that it experiences two extra interface reflections and two extra transits through the sample; therefore, the diffraction corrected ratio, r_{p1} , of the reflected to first transmitted signal is

$$r_{p1} = R_{SN}^2 e^{-2ikl} \quad (11)$$

Once R_{SN} is calculated using Eq. (11), $F(\omega)$ and CR are determined, as before. Table III presents the results for the polystyrene sample.

TABLE III. Results of polystyrene coupling experiments.

Frequency, MHz	r_{pl}	R_{SN}	$1/F(\omega)$ $10^{-14} s^2 m^2 / kg$	CR
50 kPa				
0.732	0.107e-19.473	-0.328e1.206	4.47e-10.95	0.198
0.977	0.117e-112.555	-0.342e1.212	3.78e-10.96	0.223
1.221	0.126e-116.078	-0.355e1.198	3.32e-11.02	0.245
1.465	0.131e-119.393	-0.361e1.187	2.89e-11.05	0.256
1.709	0.135e-122.639	-0.368e1.212	2.61e-10.99	0.270
79 kPa				
0.732	0.064e-19.535	-0.253e1.174	1.91e-1.75	0.085
0.977	0.065e-112.849	-0.256e1.165	1.46e-1.81	0.086
1.221	0.070e-116.145	-0.265e1.164	1.33e-1.87	0.097
1.465	0.074e-119.430	-0.271e1.169	1.21e-1.89	0.107
1.709	0.075e-122.671	-0.274e1.196	1.12e-1.82	0.115
137 kPa				
0.732	0.051e-19.624	-0.226e1.127	1.04e-1.60	0.046
0.977	0.051e-112.948	-0.226e1.116	0.73e-1.64	0.043
1.221	0.054e-116.248	-0.233e1.113	0.68e-1.80	0.051
1.456	0.057e-119.515	-0.240e1.128	0.68e-1.80	0.060
1.709	0.058e-122.720	-0.234e1.172	0.61e-1.55	0.063
362 kPa				
0.732	0.047e-19.939	-0.216e-1.028	0.41e+10.11	0.018
0.977	0.038e-113.093	-0.193e+1.033	0.24e+11.00	0.014
1.221	0.030e-116.658	-0.174e-1.093	0.56e-11.10	0.041
1.465	0.039e-119.970	-0.197e-1.101	0.30e-10.37	0.026
1.709	0.041e-122.670	-0.202e+1.097	0.24e+10.10	0.025

As with the aluminum foil testing, the value of CR drops rapidly with pressure, indicating that pressure is an effective means for improving coupling. The Table II and III values of $1/F(\omega)$ and CR are in the same ball park when compared at common pressure and frequency. In the polystyrene experiment, the magnitude of the reflected signal decreases as coupling is improved. At the

highest pressure, it is approaching the magnitude of the noise in the system, and these results are thereby less regular and less repeatable.

The results of the same experiment with a lossy, 2705 μm Kynar sample are reported in Table IV. This time, the high-pressure and high-frequency reflected signals are barely above the noise level, and only the measurements below 1.709 MHz and at 50 or 79 kPa are reported.

TABLE IV. Results of Kynar coupling experiments.

Frequency, MHz	r_{pl}	RSN	$1/F(w)$ $10^{-14} \text{s}^2 \text{m}^2 / \text{kg}$	CR
50 kPa				
0.732	$0.151e^{-112.503}$	$-0.469e^{i.109}$	$3.95e^{-11.12}$	0.199
0.977	$0.144e^{-116.518}$	$-0.508e^{i.163}$	$4.35e^{-10.95}$	0.292
1.221	$0.118e^{-120.631}$	$-0.511e^{i.136}$	$3.42e^{-11.06}$	0.288
1.465	$0.099e^{-124.806}$	$-0.522e^{i.076}$	$3.02e^{-11.35}$	0.306
79 kPa				
0.732	$0.105e^{-112.417}$	$-0.391e^{i.152}$	$1.63e^{-10.31}$	0.082
0.977	$0.106e^{-116.445}$	$-0.436e^{i.199}$	$2.35e^{-10.54}$	0.158
1.221	$0.101e^{-120.566}$	$-0.473e^{i.169}$	$2.50e^{-10.84}$	0.211
1.465	$0.091e^{-124.783}$	$-0.500e^{i.088}$	$2.46e^{-11.09}$	0.250

The values and trends in Table IV are similar to those in Table III.

VII. CONCLUSIONS

The preceding measurements and discussions were intended to show that acceptable acoustic coupling can be accomplished with soft neoprene-faced transducers. An instrument that provides repeatable, uniform contact of the transducers to the sample must be employed, and the coupling quality can be degraded by surface roughness and surface contamination. However, if sufficient pressure is applied, perfect coupling can be approached, and a means can be developed for

nondestructive testing without the drawbacks of viscous fluids, epoxies, or sample immersion. The graphs and tables were presented to give prospective users of neoprene coupling guidance for selecting reasonable operating conditions.

VII. REFERENCES

1. C. Habeger, R. Mann, and G. Baum, *Ultrasonics* 17(2), 57 (1979).
2. C. Habeger and W. Whitsitt, *Fibre Sci. and Tech.* 19, 215 (1983).
3. C. Habeger and W. Wink, *J. Appl. Polymer Sci.* 32, 4503 (1986).
4. W. Wink and G. Baum, *Tappi* 66(9), 131 (1983).
5. K. Hardacker, The Institute of Paper Chemistry, Technical Paper Series Number 138, (1984).
6. E. Papadakis, *J. Acoust. Soc. Am.* 40, 863 (1966).
7. P. Nagy and L. Adler, *J. Acoust. Soc. Am.* 82(1), 193 (1987).
8. V. Twersky, *J. Acoust. Soc. Am.* 29, 209 (1957).

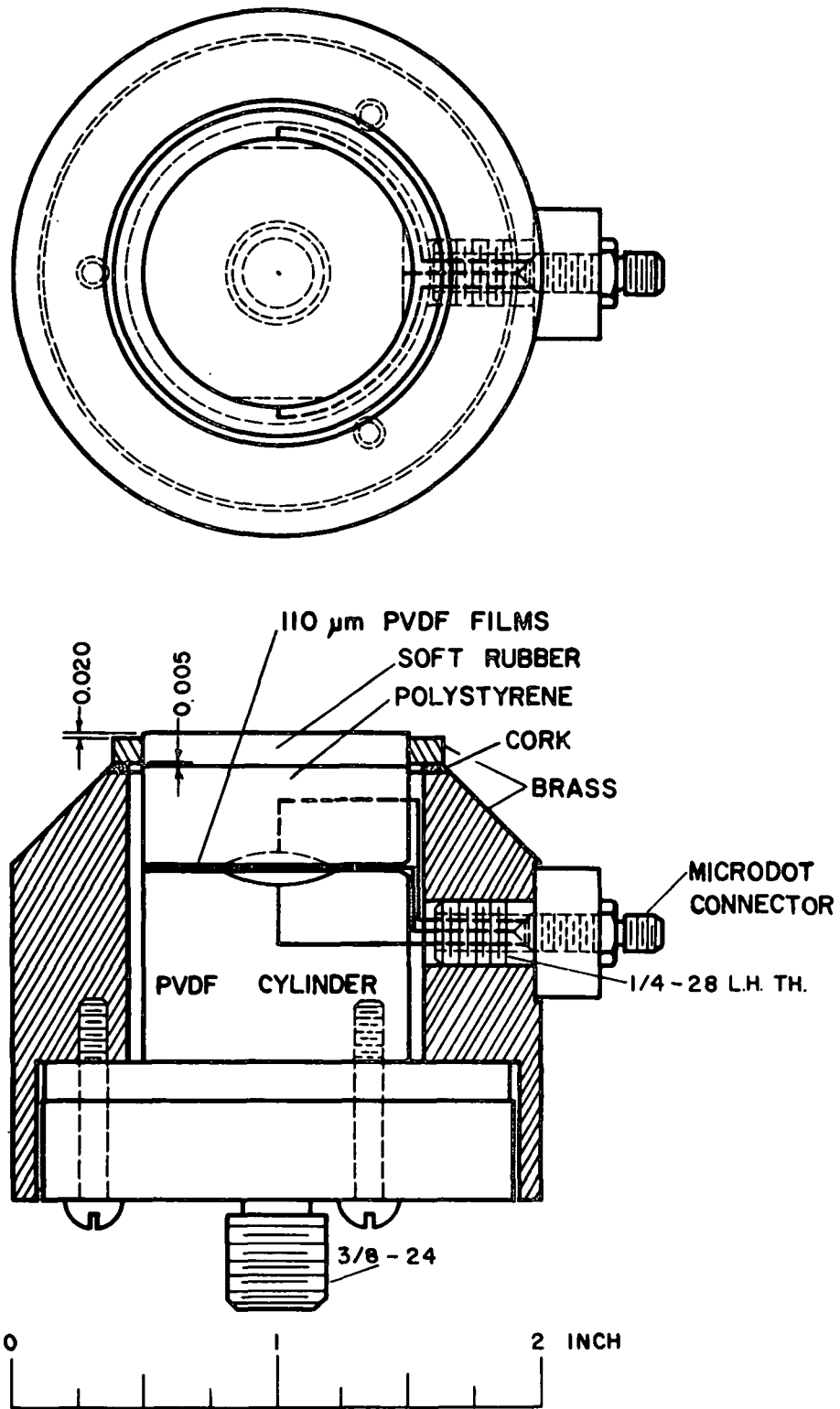


FIG. 1. Mechanical drawing for the low-impedance, neoprene-faced transducers.

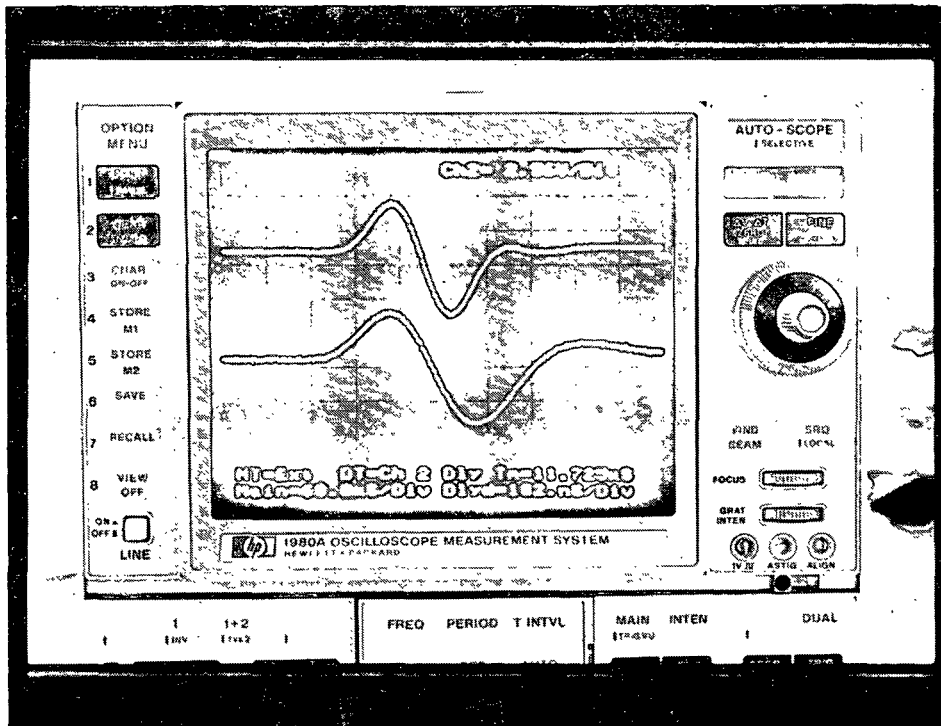


FIG. 2. Oscilloscope traces through transmissions for the two PVDF transducers.

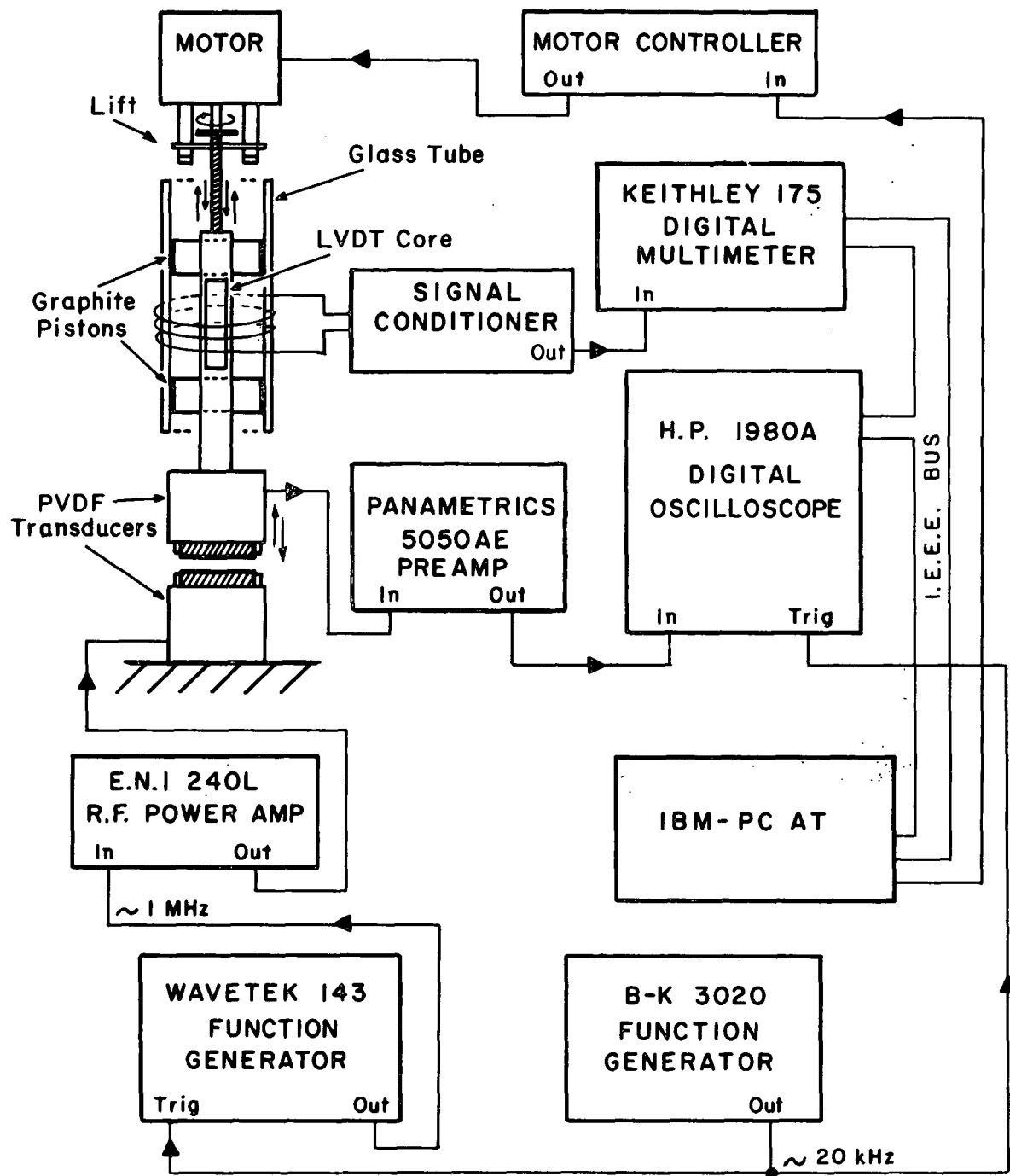


FIG. 3. Schematic diagram of the ultrasonic testing apparatus.

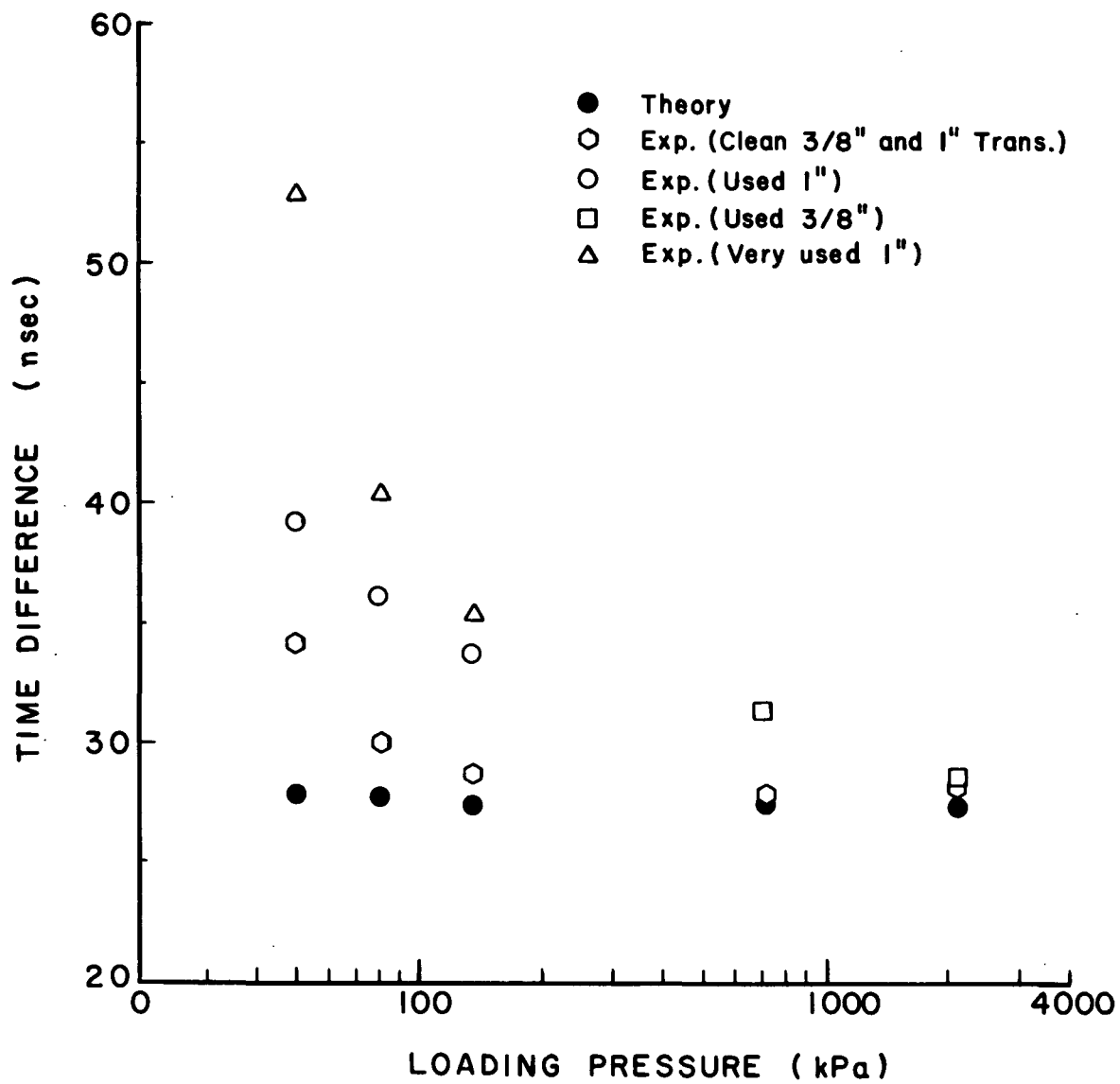


FIG. 4. Time differences through aluminum foils are a function of coupling conditions.

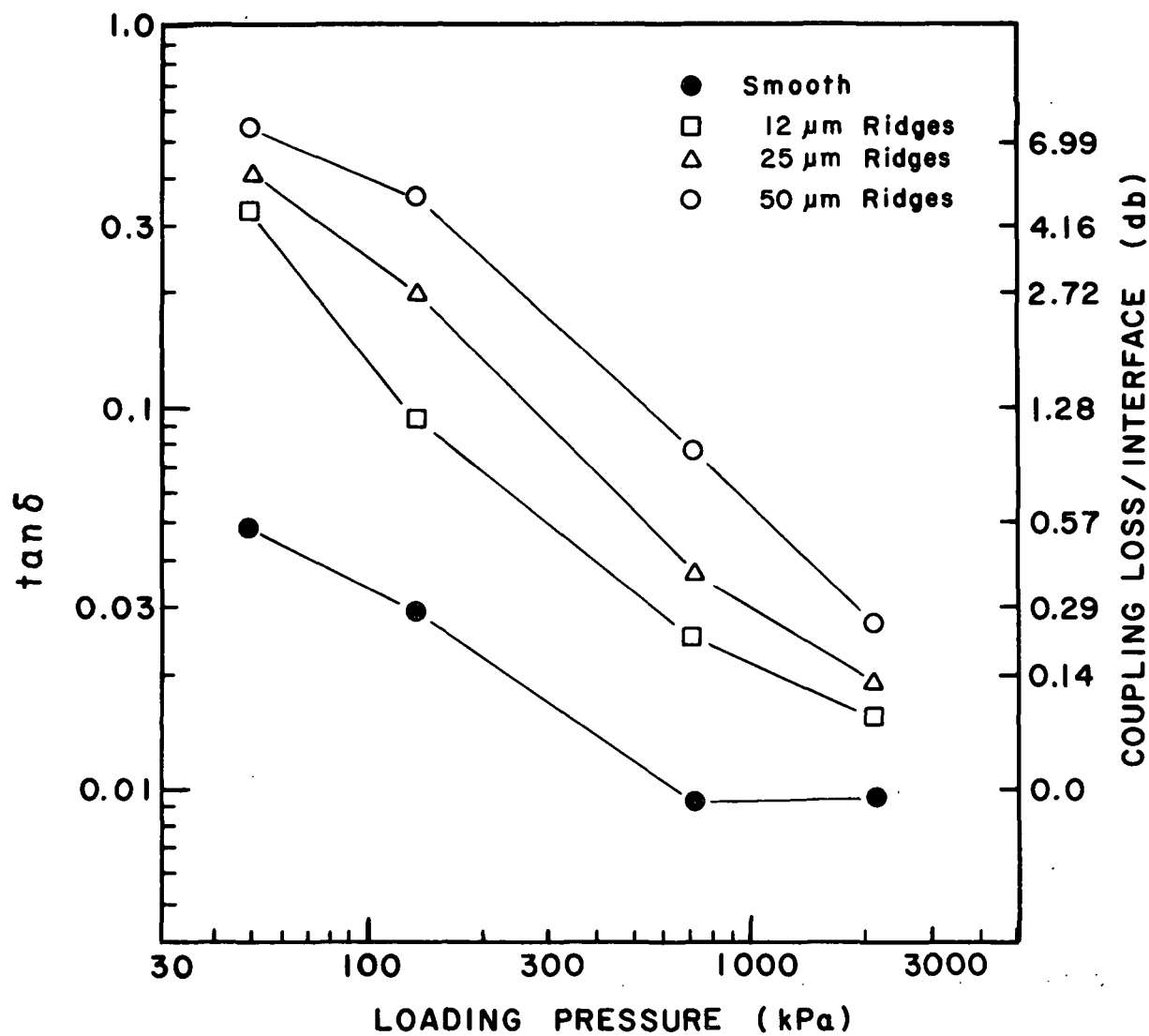


FIG. 5. The effect of loading pressure on loss tangent calculations in polystyrene.

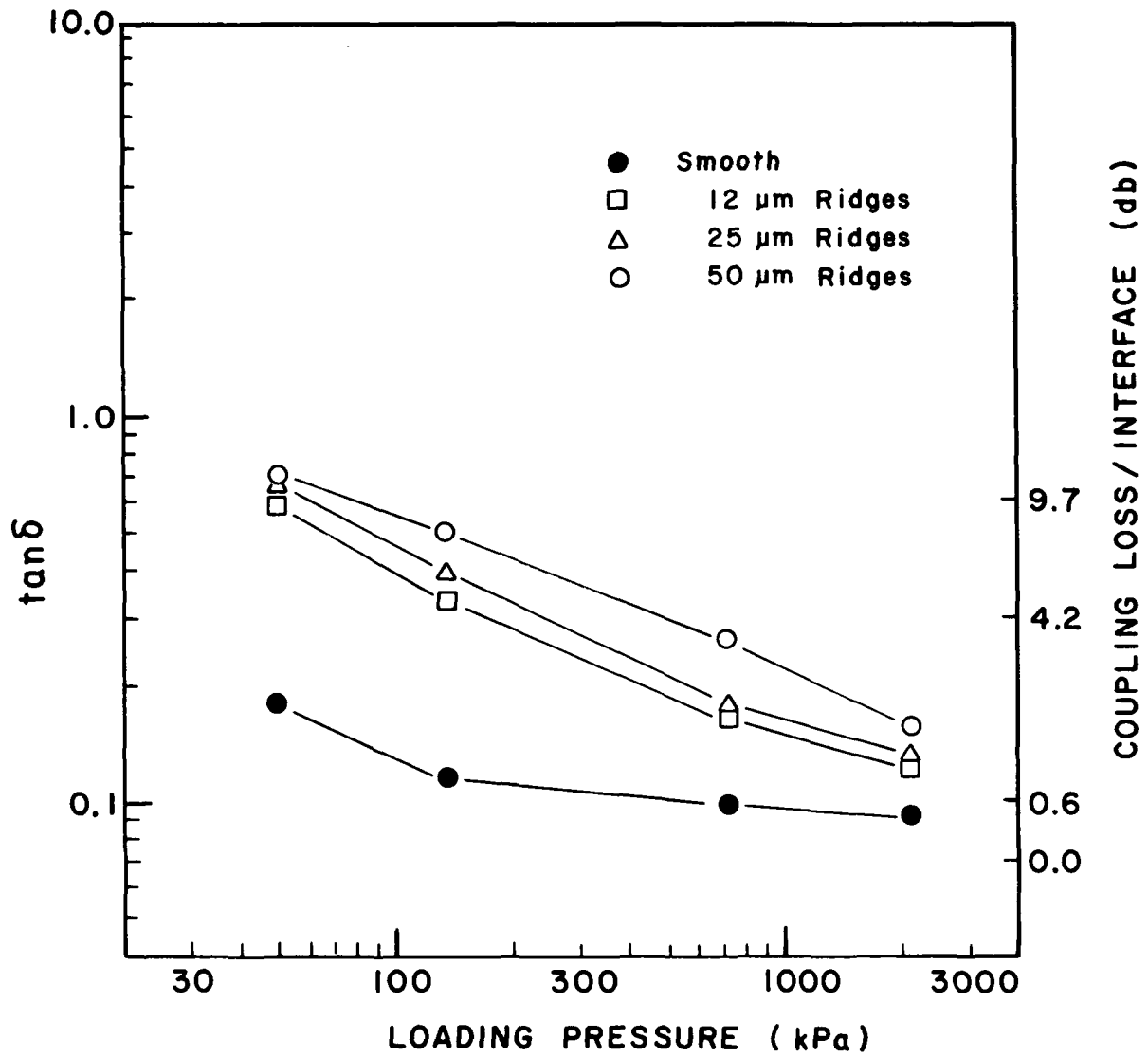


FIG. 6. The effect of loading pressure on loss tangent calculations in Kynar.